Journal of Non-Crystalline Solids 536 (2020) 120004

Contents lists available at ScienceDirect

Journal of Non-Crystalline Solids

journal homepage: www.elsevier.com/locate/jnoncrysol

Magnetocaloric effect in ercu-based metallic glass composite

Jingqing Feng[a,b], Fengmei Li[a,b], Gang Wang[a], Jun-Qiang Wang[b,*], Juntao Huo[b,*]

[a] School of Materials Science and Engineering, Shanghai University, Shanghai 200444, China
[b] CAS Key Laboratory of Magnetic Materials and Devices, and Zhejiang Province Key Laboratory of Magnetic Materials and Application Technology, Ningbo Institute of Materials Technology & Engineering, Chinese Academy of Sciences, Ningbo, Zhejiang 315201, China

ARTICLE INFO

Keywords:
Metallic glass
Magnetocaloric effect
Antiferromagnetic coupling

ABSTRACT

In order to reduce the worsen effects of strong antiferromagnetic coupling between Er and Fe, Co, Ni elements on the magnetocaloric effect of Er based amorphous alloys, an $Er_{45}Cu_{45}Al_{10}$ metallic glass composite is fabricated and its magnetocaloric effect is studied. The alloy exhibits large magnetic entropy change (14.6 $Jkg^{-1}K^{-1}$) and high refrigerant capacity (330 Jkg^{-1}) under a magnetic field of 5 T, which is a promising candidate for a magnetic refrigerant in helium liquefaction temperature range. It is intriguing that the entropy change normalized to the rare earth elements for this $Er_{45}Cu_{45}Al_{10}$ alloy is much higher than other Er-based metallic glasses, which is attributed to the weaker antiferromagnetic interactions between Er and Cu. These results are helpful for designing advanced rare earth-based magnetocaloric materials.

1. Introduction

Magnetic refrigeration is a promising solid refrigeration technology, with the outstanding advantages of environmental protection, high efficiency and small volume compared with conventional gas refrigeration [1, 2]. The magnetocaloric effect (MCE) is the principle of magnetic refrigeration. The magnetic entropy decrease when a magnetic field is applied to refrigerant because the magnetic moments of refrigerant align along the magnetic field. The decrease of magnetic entropy caused the lattice entropy increase in the adiabatic condition, which increases the temperature. When the magnetic field is removed, the upon process is reversed, and the temperature decrease [2]. One of the key points for magnetic refrigeration is the development of magnetic refrigeration materials with excellent magnetocaloric properties, e. g. large magnetic entropy change (ΔS_M), wide working temperature range and large refrigerant capacity (RC).

In the past decades, lots of materials with giant magnetocaloric effect have been discovered, such as $Gd_5(Si_2Ge_2)$ [3], $MnAs_{1-x}Sb_x$ [4], La-Fe-Si [5] and Ni-Mn-Sn [6]. And a series of materials with different magnetic transition temperatures (T_{tran}) from liquid helium temperature to room temperature have been exploited. Recently, the MCEs of metallic glasses (MG) have been widely investigated [7–15], due to their attractive properties, such as wide magnetic transition temperature, large RC, outstanding mechanical properties and excellent corrosion resistance, compared with crystalline material, which makes metallic glasses hold special application potentials as magnetocaloric materials. Especially, the rare earth (RE) based metallic glasses possessing large magnetic moments and affluent magnetic structure and thus larger ΔS_M and RC, have gained great attentions [12–15]. However, it is noteworthy that most of the RE-based MGs contain Fe, Co, Ni elements, which have strong antiferromagnetic interactions with RE atoms [16–18] and suppress the MCE of RE-based materials. Therefore, reducing the antiferromagnetic interactions is probably an effective method to improve the MCE of RE-based MGs.

It is noticed that the Cu atom has much weaker antiferromagnetic interactions with RE atoms that of Fe, Co, Ni [19]. Further evidence shows the MCE of ErCuAl [20] is larger than that of ErNiAl [21] or ErFeAl [22]. Therefore, in this work, an ErCu-based, without Fe, Co, Ni elements, amorphous/nanocrystalline composite was prepared. The magnetocaloric effects of the metallic glass composite (MGC) were investigated. Results show the MCEs of ErCu-based MGC are improved, compared with Er-MGs containing Fe, Co, Ni elements.

2. Experimental

The ingots with nominal composition of $Er_{45}Cu_{45}Al_{10}$ (at%) were prepared by arc melting pure Er, Cu and Al in a Ti-gettered argon atmosphere. Then the ingots were remelted and injected onto a rapidly spinning copper roller to get the $Er_{45}Cu_{45}Al_{10}$ metallic glass composite ribbons, the linear velocity of the roller surface is 40 m/s, and the thickness of the ribbons is about 25 μm. The microstructures of the samples were verified by X-ray diffraction (XRD) using a BRUKER D8

* Corresponding authors.
E-mail addresses: jqwang@nimte.ac.cn (J.-Q. Wang), huojuntao@nimte.ac.cn (J. Huo).

https://doi.org/10.1016/j.jnoncrysol.2020.120004
Received 5 November 2019; Received in revised form 15 February 2020; Accepted 24 February 2020

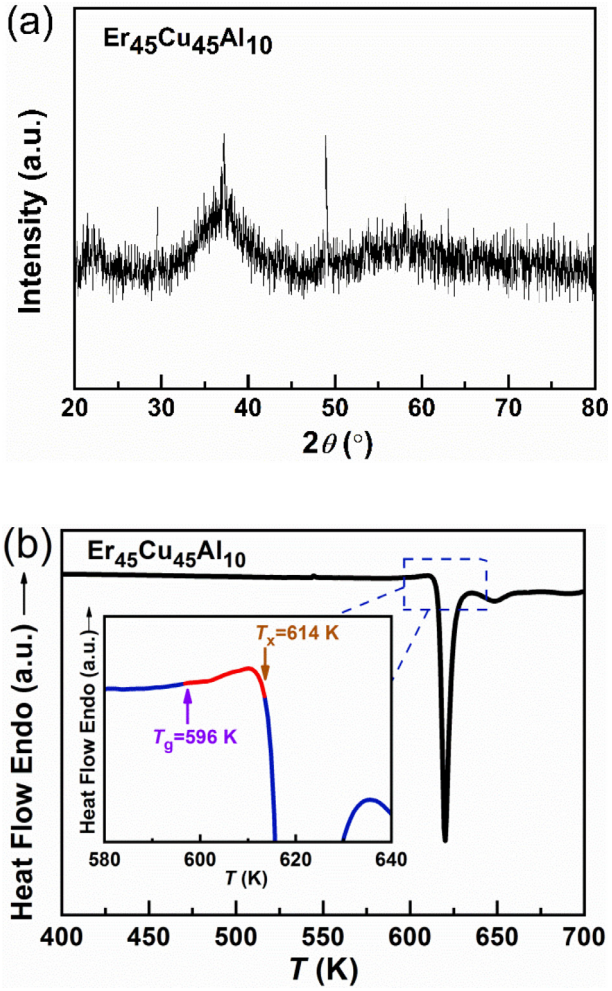

Fig. 1. (a) XRD pattern and (b) DSC trace of the as-spun $Er_{45}Cu_{45}Al_{10}$ metallic glass composite ribbons.The illustration is a magnification of the endothermic peak.

ADVANCE diffractometer with Cu Kα radiation, high-resolution transmission electron microscope (HR-TEM), selected area electron diffraction (SAED) and energy dispersive spectroscopy (EDS) using ThemoFisher Talos F200x. Thermal analysis was acquired in a NETZSCH DSC-404-C differential scanning calorimeter (DSC). The temperature and field dependence of the magnetization was measured using a SQUID magnetometer (MPMS, Quantum Design), the magnetic measurement accuracy of the SQUID magnetometer is 1×10^{-8} emu, which is very precision in the magnetic measurement.

3. Results and discussion

Fig. 1 shows the XRD pattern (Fig. 1a) and DSC traces (Fig. 1b) of the as-cast $Er_{45}Cu_{45}Al_{10}$ MGC ribbon. The XRD pattern in Fig. 1(a) exhibits appreciable crystalline peaks superimposing in the broad diffraction peaks, which indicates the alloy contains both amorphous phase and crystalline phases. But the feeble crystalline peaks can not be identified through XRD pattern, so further confirmation by transmission electron microscope will be provided later. The amorphous phase is further confirmed by DSC as shown in Fig. 1(b). In the process of heating up, the glass transition result in an endothermic reaction and the crystallization result in the exothermic peaks, the red part of curve in the illustration is the endothermic peak. The glass transition temperature (T_g), first crystallization temperature (T_x) and supercooled liquid region ($\Delta T_x = T_x - T_g$) at the heating rate of 20 K/min are 596 K, 614 K and 18 K, respectively. The small ΔT_x indicates a limited glass forming ability of this alloy, which may be why this alloy can not form complete an amorphous structure.

The HR-TEM, SAED and EDS mapping were used to further characterize the microstructures of the MGC, as shown in Fig. 2. The HR-TEM image is a light field image, the random atoms constitute the amorphous phase and thenanocrystalline phases uniformly distributed in amorphous matrix. According to the interplanar spacing of the lattice fringe and the SAED image, the nanocrystalline can be grouped into two categories, ErCuAl and Al_4Cu_9. The EDS mapping images show that the Al element distribute uniformly, but the Er and Cu element exhibit heterogeneous distributions in nanoscale. These results confirm the microstructure of the alloy is the nanocrystalline ErCuAl and Al_4Cu_9 phases distributed in amorphous matrix.

Fig. 3(a) shows the temperature dependence of the magnetization (M-T) for the $Er_{45}Cu_{45}Al_{10}$ MGC. The zero field cooling (ZFC) curve was

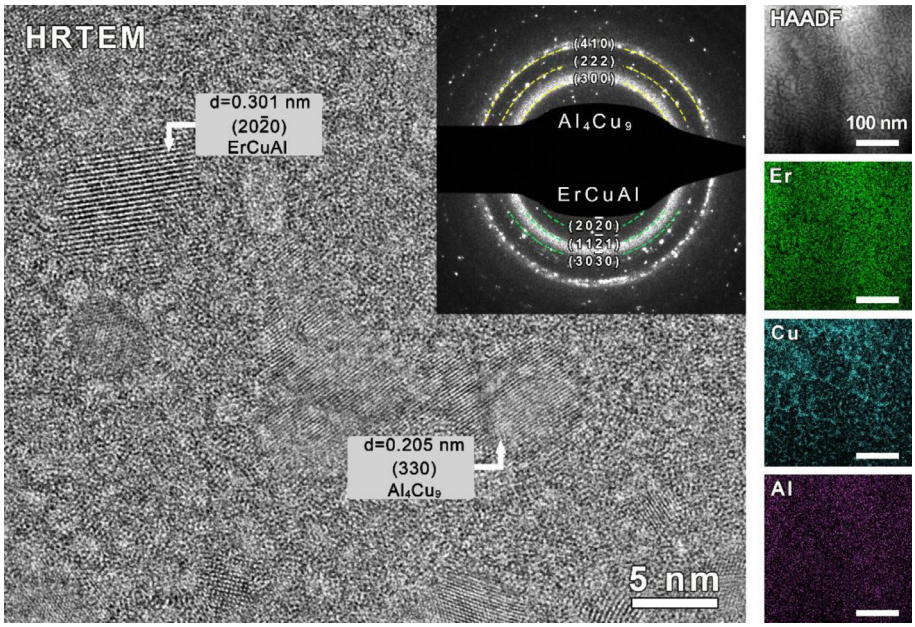

Fig. 2. The HR-TEM image of $Er_{45}Cu_{45}Al_{10}$ ribbon. The inset is the SAED. The HAADF and the EDS mapping images are shown on the right.

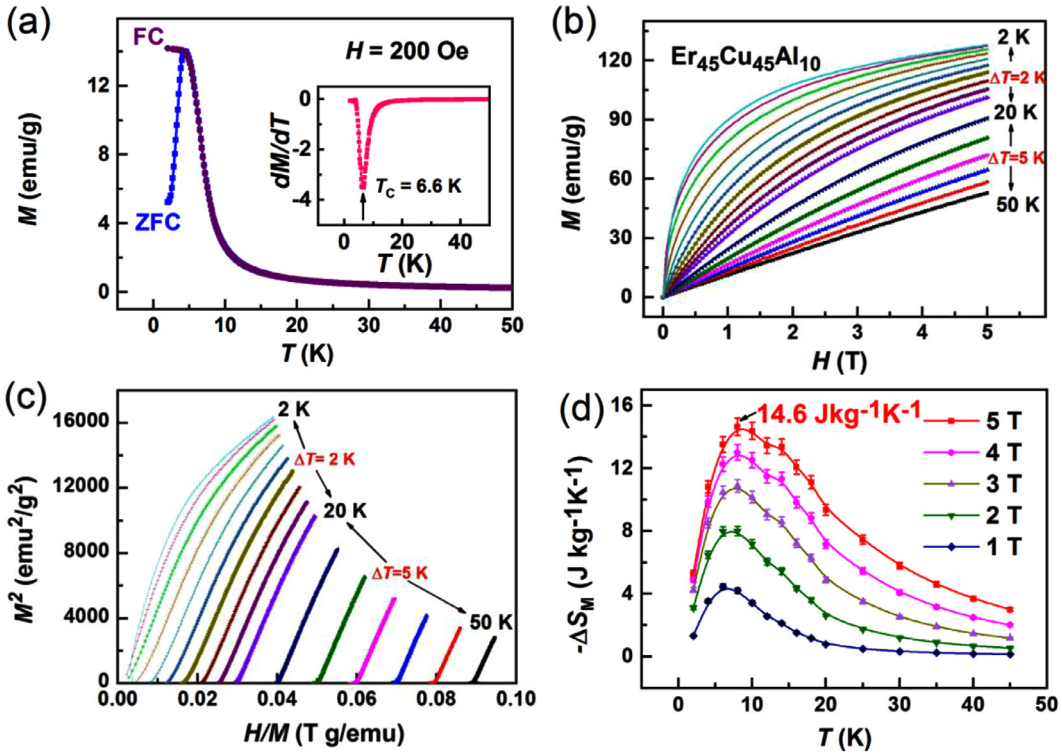

Fig. 3. (a) Temperature dependence of the zero field cooling (ZFC) and field cooling (FC) magnetization under a magnetic field of 200 Oe for the $Er_{45}Cu_{45}Al_{10}$ metallic glass composite. The inset presents the *dM/dT* versus temperature curves. (b) Isothermal magnetization curves, (c) Arrott plots, and (d) Magnetic entropy changes as a function of temperature under fields of 1 T, 2 T, 3 T, 4 T and 5 T for the $Er_{45}Cu_{45}Al_{10}$ metallic glass composite measured at temperatures between 2 K and 50 K. Temperature intervals of 2 K and 5 K were selected for the regions 2~20 K and 20~50 K, respectively, the error bars resluting from the MPMS instrument error.

measured after cooling from 300 to 2 K under zero field, and the field cooling (FC) curve was measured after cooling from 300 to 2 K under 200 Oe. The magnetization of the sample was measured in an applied field of 200 Oe from 2 K to 50 K. The ZFC curve and FC curve split off below about 4 K, the FC stays the platform while the ZFC drops sharply with the temperature decreasing, which is the characteristics of spin glass like behavior [23]. The magnetic transition temperatures (T_{tran}) of the MGC calculated from the differentiation of FC curve is 6.6 K, as is marked by arrows in the insert of Fig. 3(a). It is notable there is only one magnetic transition temperature, which is possibly because the magnetic moments of the two nanocrystalline phases are completely compled with the amorphous matrix.

Isothermal *M-H* curves with increasing filed at diverse temperatures (T_i) are shown in Fig. 3(b). To get the precise value of MCE, the temperature interval is set to be 2 K from 2 K to 20 K, and 5 K from 20 K to 50 K. The order of magnetic phase transition can be determined by the slope of Arrott plot [24], which is a plot of M^2 against H/M at fix temperatures, where M^2 is the square of the magnetization and the H/M is the ratio of the applied magnetic field to magnetization. The negative slope indicates the first order phase transition and the positive slope indicates the second order phase transition. The Arrott plot for the $Er_{45}Cu_{45}Al_{10}$ MGC sample in Fig. 3(c) shows positive slopes, indicating a second order magnetic transition.

The magnetic entropy change (ΔS_M) is an important parameter to characterize the MCE of magnetocaloric materials. In an isothermal process of magnetization, the change of applied magnetic field (H) leads to the magnetic entropy change (ΔS_M). The ΔS_M can be derived from Maxwell relation by integrating over the magnetic field [15]:

$$\Delta S_M(T, H) = \int_{H\,min}^{H\,max} \left(\frac{\partial M}{\partial T}\right)_H dH \quad (1)$$

where H_{min} and H_{max} are the initial and final values of the applied field, and the $H_{min} = 0$ and $H_{max} = 5$ T in this work. To derive the temperature dependence of ΔS_M, the numerical approximation of the integral for Eq. (1) is applied:

$$\Delta S_M(T, H) = \frac{\int_0^H M(T_i, H)dH - \int_0^H M(T_{i+1}, H)dH}{T_i - T_{i+1}} \quad (2)$$

Fig. 3(d) shows the ΔS_M as the function of the temperature under various magnetic fields for $Er_{45}Cu_{45}Al_{10}$ MGC. The peak value of magnetic entropy changes $|\Delta S_M^{pk}|$ under applied fields of 1–5 T are 4.2 $Jkg^{-1}K^{-1}$, 8.0 $Jkg^{-1}K^{-1}$, 10.9 $Jkg^{-1}K^{-1}$, 13.0 $Jkg^{-1}K^{-1}$, and 14.6 $Jkg^{-1}K^{-1}$, respectively. Table 1 lists the magnetocaloric parameters of the $Er_{45}Cu_{45}Al_{10}$ MGC and some other reported Er-based MGs [12,13,15,25–32]. It is obvious the $|\Delta S_M^{pk}|$ of the $Er_{45}Cu_{45}Al_{10}$ MGC is comparable to that of the other Er-based MGs. It is worthy noting that the rare earth element content is less than the other Er-based MGs. Therefore, the magnetic entropy change normalized by the rare earth elements $\frac{|\Delta S_M^{pk}|}{RE\ atom}$ for $Er_{45}Cu_{45}Al_{10}$ MGC is much higher than the other Er-based MGs containing Fe, Co or Ni atoms. This is attributed to the antiferromagnetic interactions in ErCu-based MGC are much weaker than that of the other Er-based MGs containing Fe, Co or Ni atoms.

Another important parameter to characterize the MCE of the MGC is the refrigerant capacity (RC), which can be measured by several kinds of methods. In this work, the RC was calculated by the product of the peak entropy change and the full width at half-maximum of the peak (δT_{FWHM}) [33], $RC = |\Delta S_M^{pk}| \times \delta T_{FWHM}$. The RC values of MGC are calculated to be 35 Jkg^{-1}, 115 Jkg^{-1},180 Jkg^{-1}, 250 Jkg^{-1}, 330 Jkg^{-1} at 1–5 T applied fields respectively.

Fig. 4.

For further understanding of the relationship of MCE and magnetic field, the magnetic field dependences of $|\Delta S_M^{pk}|$ and RC for MGC are shown in Fig. 5. The universal relations have been deduced to be $|\Delta S_M^{pk}| \propto H^n$ and $RC \propto H^N$ [34,35]. n and N are the critical exponents of the metallic glass composite in this paper, which can be obtained from the

Table 1

Magnetic transition temperature T_{tran}, the peak value of magnetic entropy change $|\Delta S_M^{pk}|$, the $|\Delta S_M^{pk}|$ normalized by the rare earth elements $\frac{|\Delta S_M^{pk}|}{\text{RE atom}}$, refrigerant capacity RC under a maximum applied field of 5 T of the $Er_{45}Cu_{45}Al_{10}$ metallic glass composite and some other Er-based metallic glasses.

NO.	Composition	T_{tran} (K)	$\lvert\Delta S_M^{pk}\rvert$ ($Jkg^{-1}K^{-1}$)	$\frac{\lvert\Delta S_M^{pk}\rvert}{\text{RE atoms}}$	RC (Jkg^{-1})	Ref.
1	$Er_{45}Cu_{45}Al_{10}$	6.6	14.6	0.324	330	This work
2	$Er_{65}Co_{30}$	12.5	5.97	0.091	–	[25]
3	$Er_{56}Al_{24}Co_{20}$	9	16.06	0.286	546	[26]
4	$Er_{60}Al_{18}Co_{22}$	12	17.6	0.293	546	[27]
5	$Er_{60}Ni_{30}Co_{10}$	11.5	12.1	0.201	–	[28]
6	$Er_{50}Co_{20}Al_{24}Y_6$	8	15.91	0.284	423	[13]
7	$Er_{60}Al_{16}Co_{20}Ni_4$	11	16.5	0.275	326	[29]
8	$Er_{22}Gd_{33}Al_{25}Co_{20}$	52	9.47	0.172	574	[12]
9	$Er_{48}Tm_8Co_{24}Al_{20}$	11	16	0.285	–	[30]
10	$Er_{32}Tm_{24}Co_{24}Al_{20}$	7.5	17	0.303	–	[30]
11	$Er_4Gd_{48}Al_{25}Co_{20}Zr_3$	84	9.41	0.180	647	[31]
12	$(Er_{0.7}Ho_{0.2}Dy_{0.1})_{55}Ni_{25}Al_{20}$	5	14.02	0.254	277	[15]
13	$Er_{0.2}Gd_{0.2}Ho_{0.2}Co_{0.2}Cu_{0.2}$	49	11.1	0.185	649	[32]

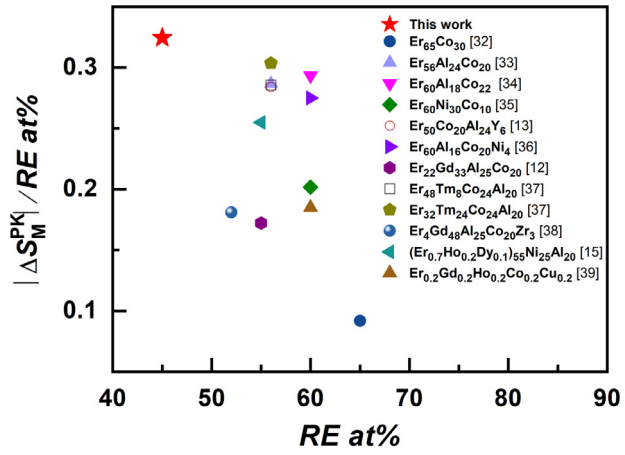

Fig. 4. The magnetic entropy normallized by the rare earth atoms versus the concentration of RE elements for different RE-based magnetocaloric materials.

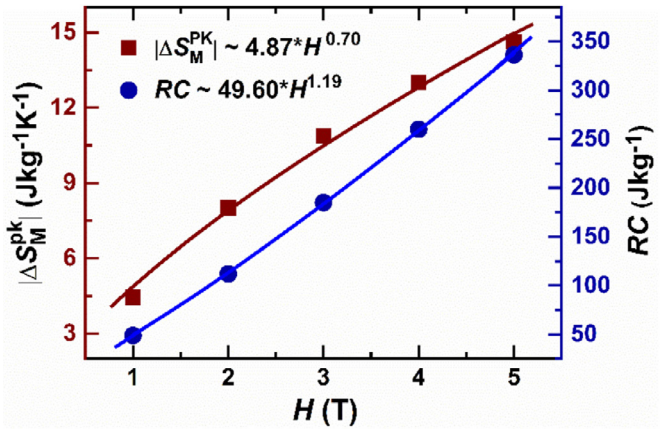

Fig. 5. Magnetic field dependence of the maximum magnetic entropy change ($|\Delta S_M^{pk}|$), and refrigerant capacity (RC) for the $Er_{45}Cu_{45}Al_{10}$ metallic glass composite. The solid curves are fitting results of $|\Delta S_M^{pk}| \propto aH^n$ and $RC \propto AH^N$, respectively.

fitting results of the experimental data in Fig. 5. For the MGC alloy, $n = 0.7$, and $N = 1.19$, both are close to other metallic glasses [36,37]. The theoretical value of n is ~2/3 at the transition temperature on the basis of the mean field model [38]. Nevertheless, the exponents n of MGC is larger than 2/3, which is probably due to the failure of the mean field picture in the critical region [39].

4. Conclusions

The $Er_{45}Cu_{45}Al_{10}$ metallic glass composite has been developed, which shows outstanding magnetocaloric effect . Its $|\Delta S_M^{pk}|$, T_{tran} and RC is 14.6 $Jkg^{-1}K^{-1}$, 6.6 K and 336 Jkg^{-1} respectively. Most importantly, the ΔS_M^{pk} normalized to RE atoms of the ErCu-based MGC is much larger than that of other Er-based MGs containing Fe, Co or Ni elements, attributed to the antiferromagnetic coupling interactions are inhibited. These results are meaningful to decrease the dosage of rare earth elements, and improve the magnetocaloric property of rare earth based metallic glasses.

Credit author statement

All authors listed have made a significant contribution to the research reported and have read and approved the submitted manuscript, and furthermore, all those who made substantive contributions to this work have been included in the author list.

CRediT authorship contribution statement

Jingqing Feng: Data curation, Writing - original draft. **Fengmei Li:** Data curation, Writing - original draft. **Gang Wang:** Conceptualization, Methodology, Writing - review & editing. **Jun-Qiang Wang:** Conceptualization, Methodology, Writing - review & editing. **Juntao Huo:** Conceptualization, Methodology, Writing - review & editing.

Declaration of Competing Interest

The authors declare that they have no known competing financial interests or personal relationships that could have appeared to influence the work reported in this paper.

Acknowledgements

This work was supported by the National Natural Science Foundation of China (NSFC 51827801, 51771217, 51771216), Zhejiang Provincial Natural Science Foundation of China (LY17E010005), and Youth Innovation Promotion Association CAS (2019296).

References

[1] S. Uporov, V. Bykov, N. Uporova, Magnetocaloric effect in $Gd_{60}Al25(NiCo)_{15}$ bulk metallic glass, J Non Cryst Solids 521 (2019) 119506.
[2] V. Franco, J.S. Blázquez, J.J. Ipus, J.Y. Law, L.M. Moreno-Ramírez, A. Conde, Magnetocaloric effect: from materials research to refrigeration, Prog Mater Sci 93 (2018) 112–232.
[3] V.K. Pecharsky, J.K.A. Gschneidner, Giant magnetocaloric effect in $Gd_5Si_2Ge_2$,

Phys. Rev. Lett. 78 (1997) 4494–4497.
[4] H. Wada, Y. Tanabe, Giant magnetocaloric effect of mnas$_{1-x}$ sb$_x$, Appl Phys Lett 79 (2001) 3302–3304.
[5] X. Chen, Y.G. Chen, Y.B. Tang, D.Q. Xiao, Effects of the excess iron on phase and magnetocaloric property of lafe$_{11.6x}$ Si$_{1.4}$ alloys, Journal of Rare Earths 33 (2015) 1293–1297.
[6] T. Krenke, E. Duman, M. Acet, E.F. Wassermann, X. Moya, L. Manosa, A. Planes, Inverse magnetocaloric effect in ferromagnetic ni-mn-sn alloys, Nat Mater 4 (2005) 450–454.
[7] J.T. Huo, W. Sheng, J.Q. Wang, Magnetocaloric effects and magnetic regenerator performances in metallic glasses, Acta Physica Sinica 66 (2017) 307–324.
[8] S. Atalay, H. Gencer, V.S. Kolat, Magnetic entropy change in Fe$_{74-x}$ cr$_x$cu$_1$nb$_3$si$_{13}$b$_9$ (x = 14 and 17) amorphous alloys, J Non Cryst Solids 351 (2005) 2373–2377.
[9] V. Franco, J.S. Blázquez, A. Conde, The influence of co addition on the magnetocaloric effect of nanoperm-type amorphous alloys, J Appl Phys 100 (2006) 064307.
[10] V. Franco, J.M. Borrego, A. Conde, S. Roth, Influence of co addition on the magnetocaloric effect of fecosialgapcb amorphous alloys, Appl Phys Lett 88 (2006) 132509.
[11] T.D. Shen, R.B. Schwarz, J.Y. Coulter, J.D. Thompson, Magnetocaloric effect in bulk amorphous Pd$_{40}$Ni$_{22.5}$Fe$_{17.5}$P$_{20}$ alloy, J Appl Phys 91 (2002) 5240–5245.
[12] Q. Luo, D.Q. Zhao, M.X. Pan, W.H. Wang, Magnetocaloric effect in gd-based bulk metallic glasses, Appl Phys Lett 89 (2006) 081914.
[13] Q. Luo, D.Q. Zhao, M.X. Pan, W.H. Wang, Magnetocaloric effect of ho-, dy-, and er-based bulk metallic glasses in helium and hydrogen liquefaction temperature range, Appl Phys Lett 90 (2007) 211903.
[14] J.T. Huo, D.Q. Zhao, H.Y. Bai, E. Axinte, W.H. Wang, Giant magnetocaloric effect in tm-based bulk metallic glasses, J Non Cryst Solids 359 (2013) 1–4.
[15] Q. Luo, W.H. Wang, Magnetocaloric effect in rare earth-based bulk metallic glasses, J Alloys Compd 495 (2010) 209–216.
[16] D. Coffey, J.L. Diez-Ferrer, D. Serrate, M. Ciria, C. de la Fuente, J.I. Arnaudas, Antiferromagnetic spin coupling between rare earth adatoms and iron islands probed by spin-polarized tunneling, Sci Rep 5 (2015) 13709.
[17] R. Kirsch, M.J. Prandolini, M. Gierlings, M. Gruyters, W.D. Brewer, D. Riegel, Implantation of single-impurity fe and its magnetic coupling in er studied by tdpad, J Magn Magn Mater 272–276 (2004) 760–761.
[18] J. Tang, Y.J. Ke, W. He, X.Q. Zhang, W. Zhang, N. Li, Y.S. Zhang, Y. Li, Z.H. Cheng, Ultrafast photoinduced multimode antiferromagnetic spin dynamics in exchange-coupled fe/rfeo$_3$ (R = er or dy) heterostructures, Advanced Materials 30 (2018) 1706439.
[19] R.C. Sherwood, H.J. Williams, J.H. Wernick, Metamagnetism of some rare-earth copper compounds with cecu$_2$ structure, J Appl Phys 35 (1964) 1049–1050.
[20] Q.Y. Dong, J. Chen, J. Shen, J.R. Sun, B.G. Shen, Large magnetic entropy change and refrigerant capacity in rare-earth intermetallic RCuAl (R = Ho and er) compounds, J Magn Magn Mater 324 (2012) 2676–2678.
[21] B.J. Korte, V.K. Pecharsky, K.A. Gschneidner Jr., The correlation of the magnetic properties and the magnetocaloric effect in (Gd1-xErx)NiAl alloys, J Appl Phys 84 (1998) 5677–5685.
[22] Y.K. Zhang, G. Wilde, X. Li, Z.M. Ren, L.W. Li, Magnetism and magnetocaloric effect in the ternary equiatomic REFeAl (RE = Er and ho) compounds, Intermetallics 65 (2015) 61–65.
[23] J.T. Huo, Q. Luo, J.Q. Wang, W. Xu, X. Wang, R.W. Li, H.B. Yu, Nonlinear fragile-to-strong transition in a magnetic glass system driven by magnetic field, AIP Adv 7 (2017) 125014.
[24] J.Y. Fan, L.S. Ling, B. Hong, L. Zhang, L. Pi, Y.h. Zhang, Critical properties of the perovskite manganite La$_{0.1}$Nd$_{0.6}$Sr$_{0.3}$MnO$_3$, Physical Review B 81 (2010) 144426.
[25] A. Boutahar, H. Lassri, K. Zehani, L. Bessais, E.K. Hlil, Magnetic properties and magnetocaloric effect in amorphous Co$_{35}$Er$_{65}$ ribbon, J Magn Magn Mater 369 (2014) 92–95.
[26] X.D. Hui, Z.Y. Xu, Y. Wu, X.H. Chen, X.J. Liu, Z.P. Lu, Magnetocaloric effect in er-al-co bulk metallic glasses, Chinese Science Bulletin 56 (2011) 3978–3983.
[27] X.D. Hui, Z.Y. Xu, E.R. Wang, G.L. Chen, Z.P. Lu, Excellent magnetocaloric effect in Er$_{60}$Al$_{18}$Co$_{22}$ bulk metallic glass, Chinese Physics Letters 27 (2010) 117502.
[28] W.L. Gao, X.J. Wang, L.J. Wang, Y.K. Zhang, J.Z. Cui, Cryogenic magnetic properties of Er$_{60}$Ni$_{30}$Co$_{10}$ amorphous ribbon, J Non Cryst Solids 484 (2018) 36–39.
[29] Q. Luo, M.B. Tang, J. Shen, Tuning the magnetocaloric response of er-based metallic glasses by varying structural order in disorder, J Magn Magn Mater 401 (2016) 406–411.
[30] X.H. Kou, Q. Luo, P.N. Dinh, J. Shen, Magnetocaloric response and its power law relationship with magnetoresistance in er-tm-co-al metallic glasses, J Alloys Compd 699 (2017) 591–595.
[31] W.H. Wang, Bulk metallic glasses with functional physical properties, Advanced Materials 21 (2009) 4524–4544.
[32] L.W. Li, C. Xu, Y. Yuan, S.Q. Zhou, Large refrigerant capacity induced by table-like magnetocaloric effect in amorphous Er$_{0.2}$Gd$_{0.2}$Ho$_{0.2}$Co$_{0.2}$Cu$_{0.2}$ ribbons, Materials Research Letters 6 (2018) 413–418.
[33] M.E. Wood, W.H. Potter, General analysis of magnetic refrigeration and its optimization using a new concept: maximization of refrigerant capacity, Cryogenics (Guildf) 25 (1985) 667–683.
[34] H. Oesterreicher, F.T. Parker, Magnetic cooling near curie temperatures above 300 K, J Appl Phys 55 (1984) 4334–4338.
[35] Y. Su, Y. Sui, J.G. Cheng, J.S. Zhou, X. Wang, Y. Wang, J.B. Goodenough, Critical behavior of the ferromagnetic perovskites RTiO$_3$ (R = Dy, ho, er, tm, yb) by magnetocaloric measurements, Physical Review B 87 (2013) 195102.
[36] J.T. Huo, L. Huo, J. Li, H. Men, X. Wang, A. Inoue, C. Chang, J.Q. Wang, R.W. Li, High-entropy bulk metallic glasses as promising magnetic refrigerants, J Appl Phys 117 (2015) 073902.
[37] J.T. Huo, J.Q. Wang, W.H. Wang, Denary high entropy metallic glass with large magnetocaloric effect, J Alloys Compd 776 (2019) 202–206.
[38] V. Franco, C.F. Conde, J.S. Blázquez, A. Conde, P. Švec, D. Janičkovič, L.F. Kiss, A constant magnetocaloric response in femocub amorphous alloys with different fe/b ratios, J Appl Phys 101 (2007) 093903.
[39] Q. Luo, B. Schwarz, N. Mattern, J. Shen, J. Eckert, Roles of hydrogenation, annealing and field in the structure and magnetic entropy change of tb-based bulk metallic glasses, AIP Adv 3 (2013) 032134.